

Uncertainty of Aircraft Localization with Multilateration and Known Altitude

Osypiuk, Rafał; Surma, Filip

DOI

[10.3390/electronics14122420](https://doi.org/10.3390/electronics14122420)

Publication date

2025

Document Version

Final published version

Published in

Electronics (Switzerland)

Citation (APA)

Osypiuk, R., & Surma, F. (2025). Uncertainty of Aircraft Localization with Multilateration and Known Altitude. *Electronics (Switzerland)*, 14(12), Article 2420. <https://doi.org/10.3390/electronics14122420>

Important note

To cite this publication, please use the final published version (if applicable). Please check the document version above.

Copyright

Other than for strictly personal use, it is not permitted to download, forward or distribute the text or part of it, without the consent of the author(s) and/or copyright holder(s), unless the work is under an open content license such as Creative Commons.

Takedown policy

Please contact us and provide details if you believe this document breaches copyrights. We will remove access to the work immediately and investigate your claim.

Article

Uncertainty of Aircraft Localization with Multilateration and Known Altitude

Rafał Osypiuk ^{1,*}  and Filip Surma ² 

¹ Department of Control Engineering and Robotics, West Pomeranian University of Technology Szczecin, 71126 Szczecin, Poland

² Aerospace Engineering Faculty, Delft University of Technology, 2629 HS Delft, The Netherlands; f.surma@tudelft.nl

* Correspondence: rafal.osypiuk@zut.edu.pl; Tel.: +48-500-305-700

Abstract: Manned and unmanned air traffic is experiencing rapid growth. The basis for the safety of flight operations is its reliable surveillance. In addition to primary and secondary radar, modern systems based on satellite positioning play a key role in air traffic control. An important addition to the above systems is multilateration (MLAT). The majority of existing MLAT algorithms operate under the assumption that only the time difference of arrival (TDOA) is available for consideration. However, in scenarios that are more reflective of reality, altitude measurements are also typically included. In this study, we not only extend an existing algorithm to accommodate these additional data points but also derive insights into how the accuracy of measurements is influenced by the incorporation of supplementary information. An important part of this contribution is the software, which, by solving nonlinear optimization problems, allows for the analysis of the distribution of MLAT stations while ensuring the smallest possible measurement uncertainties.

Keywords: multilateration; air traffic surveillance; localization; ADS-B



check for updates

Academic Editor: Olivier Sename

Received: 27 March 2025

Revised: 9 June 2025

Accepted: 12 June 2025

Published: 13 June 2025

Citation: Osypiuk, R.; Surma, F. Uncertainty of Aircraft Localization with Multilateration and Known Altitude. *Electronics* **2025**, *14*, 2420. <https://doi.org/10.3390/electronics14122420>

Copyright: © 2025 by the authors. Licensee MDPI, Basel, Switzerland. This article is an open access article distributed under the terms and conditions of the Creative Commons Attribution (CC BY) license (<https://creativecommons.org/licenses/by/4.0/>).

1. Introduction

Tracking airspace users is fundamental for ensuring safety in air transportation. This issue has gained importance with the rise of manned flight operations globally and the increasing number of drones in the airspace. The capabilities of primary and secondary radar are limited, and the goal is to reduce separation in air traffic. Modern systems that use GNSS (Global Navigation Satellite System) navigation in their operation are proving helpful. One such system is ADS-B (Automatic Dependent Surveillance–Broadcast), which continues to be deployed on aircraft through transformation programs such as NextGen (USA) or Single European Sky. Derivatives of the ADS-B system, such as the UAT (Universal Access Transceiver) and FLARM, are also widely adopted. The newest one is RemoteID for drones, which became legally effective in 2024 (USA and Europe). Despite these significant advances in aircraft localization systems, multilateration (MLAT) algorithms still play a key role in estimating the position of aircraft. MLAT is an important complement to secondary radar and allows the estimation of aircraft positions with precision down to a single meter. An example of this is the PHOENIX system from DFS, the German Air Navigation Service Provider, which also uses interrogating station positions to improve the precision of MLAT algorithms. MLAT also plays an important role in GNSS-based air traffic surveillance systems. However, its operation is different and involves testing the integrity of transmitted data and protecting against intentional spoofing [1]. Regardless of the end use, the core of the MLAT system remains the same.

Multilateration uses ground stations (receivers) placed in strategic locations to collect signals from aircraft (transmitters). In MLAT systems, time differences of arrival (TDOAs) are used instead of TOAs. The primary difference between the two is that, in contrast to GNSS, the former does not require knowledge of the transmission time of the signal. A TDOA is created by selecting a reference station and subtracting its TOA from the TOAs of the other stations. However, according to [2], “the algorithms for the TDOA techniques are generally more complex than other techniques such as the time of arrival, angle of arrival, and the received signal strength”. The measurement error of MLAT localization depends on the measurement time variance and the geometric arrangement of the stations. The Dilution of Precision (DOP) is a scalar value used to describe the effect of geometry on the localization error [3].

In the literature, equations have been derived to calculate the DOP for MLAT systems but have been proposed only for systems where the MLAT algorithm is the only source of localization [3–5]. In this paper, we assume that aircraft are equipped with barometric altimeters, which are very accurate compared to MLAT localization. Since the measurement of altitude is very accurate, we simplify the problem by assuming that the altitude of an aircraft is known. It should be noted, however, that the majority of algorithms presented in Section 2 were designed for Cartesian dimensions (x, y, z). In order to represent the knowledge of an altitude, it is necessary to use ENU (east–north–up) coordinates or any other coordinates based on latitude and longitude.

We also assume that most of the measurements are received passively by the MLAT system, but the interrogating station can send a query to the aircraft, which responds with an approximately known time. An example of such a system was presented in [6]. With this information, it is possible to use both TOAs and TDOAs for localization.

The paper makes the following contributions:

- We implement several nonlinear optimization problems, the solutions to which return the locations of a drone based on the available measurements. As the altitude measurements are given in a different coordinate system, this is taken into account. The results of these optimization problems are compared. Furthermore, we compare them to an existing approach, Foy’s algorithm [7], which we extend to take into account altitude measurements.
- In [3], an approach for calculating the DOP was presented. This approach is extended to consider altitude measurements. Furthermore, in the case study, the impact of both the different configurations of ground stations’ locations and the different optimization problems on the DOP over an area is demonstrated.

To demonstrate the capabilities of the proposed algorithm, software was prepared to analyze and optimize the positions of MLAT system receiving stations.

2. Related Works

To date, many algorithms have been proposed to locate transmitters based on the TDOA. They can be divided into closed and open methods [8]. Closed methods transform a set of TDOA equations into a mathematical function that relates the unknown target position to the measurements. These methods are fast, but the solutions are generally biased and not optimal in a statistical sense. Examples are presented in [9–14].

Open algorithms assume that all noise is normally distributed and try to iteratively find the position in space that minimizes the mean square error of all measurements. If convergence is achieved and the statistical hypothesis for the measurement errors is satisfied, they provide optimal estimators in the statistical sense, i.e., estimators that are practically unbiased and with performance very close to the Cramer–Rao lower bound [15]. However, open-form methods are slower and need to find a good initial estimator, which is not a

trivial problem. In [16], the authors solved this problem by using a closed algorithm to find the starting position. A machine learning starting-position-estimation algorithm was presented in [1] (see [7,17,18] for more examples of open algorithms). There are also algorithms that use measurements of both MLAT and aircraft altitude during localization ([6] (closed) and [1] (open)). However, they do not specify how certain the measurements are.

In this paper, the position is determined by employing a general-purpose solver for nonlinear optimization problems. Despite the fact that the previously mentioned approach utilizes the structure of the problem, it is not easily extendable in the event that additional information, such as altitude, is present. The utilization of a general-purpose solver facilitates the incorporation of nonlinear constraints, thereby enabling the inclusion of these elements.

In [19], the DOP was defined as the ratio of the RMS position error to the RMS range error. In [3], a method to compute it for the MLAT system was presented. It requires computing the Jacobian of the measurement equations and the covariance matrix. It is possible to compute the DOP by assuming that the variance of the measurements is equal, i.e., that each station has the same accuracy. In [4], the authors analyzed how the number of stations affects the DOP for a two-dimensional case. Table 1 from [20] shows how to interpret the DOP value.

Table 1. Interpretation of DOP values.

DOP	Rating
1	IDEAL
2–3	EXCELLENT
4–6	GOOD
7–8	MODERATE
9–20	FAIR
21<	POOR

Maximizing the DOP over a given area is an important factor in the placement of ground stations for both TOA [21] and TDOA [2,5] measurements. However, the cited approaches only indicate which placement is optimal, but in a real-world scenario, the optimal placement, e.g., a rectangle, may not be available. The software discussed in Section 4 allows for visualizing and comparing how different station placements affect the accuracy of the measurements over the selected area.

3. Proposed Method

3.1. Problem Formulation

An aircraft moves in three-dimensional space and periodically transmits its altitude without providing information on when a message was sent. The position can be represented by a three-dimensional vector $P = [lat, lon, alt]$ of latitude, longitude, and altitude. This coordinate system is not only more common in navigation than the Cartesian coordinate system but also allows us to separate the altitude from the other coordinates.

The signal is received by N ground stations that are in communication with each other. Their positions are known and can be represented by a three-dimensional vector $\bar{P}_i = [\overline{lan}_i, \overline{lot}_i, \overline{alt}_i]$, where i is the order number of the station.

Each time the aircraft sends information, a TOA measurement for each station is obtained, which is defined in (1), where T_s is the timestamp when the message was sent, n_i is the noise of the i -th measurement, and $\| \cdot \|$ is the Euclidean distance operation. We

assume that the noise is normally distributed with known variance for each station. In this paper, we consider three methods for solving this problem.

$$TOA_i = \frac{1}{c}(\|P - \bar{P}_i\|) + Ts + n_i \quad i = 1 \dots N \quad (1)$$

First, the TDOA is calculated by subtracting the TOA of the reference station from the other TOAs. This gives a set of measurements, described by (2), in which the first station is the reference station. In this case, $n_{i,1}$ is also normally distributed noise, but it has twice the variance of n_i . The TDOAs can then be used as input to the localization algorithm.

$$TDOA_{i,1} = \frac{1}{c}(\|P - \bar{P}_i\| - \|P - \bar{P}_1\|) + n_{i,1} \quad i = 2 \dots N \quad (2)$$

Second, we can treat the moment of sending a message as an additional unknown variable to be determined. Compared to the previous approach, we can directly use TOAs, which adds another equation to the system.

The last approach is to try to estimate Ts before optimization. This is possible if the aircraft responds to our query. We assume that the time taken to respond is equal to the sum of the known value Ta and the normally distributed noise n_a with known variance. If a response is received relatively quickly, we can assume that Ta is small enough to treat the distance traveled by the aircraft as being equal to 0. Ts can be estimated using (3), where Tq is a known timestamp of sending a query, and the variance of n_s is equal to the sum of the variances of n_a and n_1 . We call these measurements TOAq, i.e., TOA measurements with an additional query.

$$\bar{T}s = \frac{1}{2}(TOA_1 + Tq + Ta) + n_s \quad (3)$$

When using a presented algorithm, we often move between the east–north–up (ENU) coordinate system and the geographic (Geo) coordinate system, which uses latitude, longitude, and altitude based on equations from [22]. Geo is the most commonly used system for localization in aerospace applications. However, it is not a Cartesian coordinate system, and most MLAT algorithms have been designed with this type of coordinate system in mind. The Earth-Centered, Earth-Fixed (ECEF) coordinate system is another commonly used system. It is a Cartesian coordinate system in which the origin is the center of the Earth, the z-axis passes through true north, and the x-axis intersects the Earth at 0° latitude and longitude. However, it does not allow us to represent an altitude simply because none of the coordinates are parallel to it.

In the ENU coordinate system, the origin is not specified and can be chosen according to the needs of the application. In order to switch from Geo to ENU, it is necessary to move to ECEF [22] first. The ENU coordinate system allows us to display altitude as a z-coordinate, but only if the aircraft's position is known. This is not a problem when trying to estimate the localization error after localizing an aircraft, but during the localization procedure, the position is unknown. If an open algorithm is used, we obtain a guess in each iteration. This guess can be used as the origin, and after each iteration, the ENU coordinates are updated accordingly. Converting coordinates between different systems can be achieved through the utilization of existing software packages, such as `pymap3d` (Version: 3.1.0) [22].

Alternatively, it is possible to represent height as a nonlinear constraint instead of as a single variable. This can be done if the problem is solved using a general-purpose solver, but it is not easy to extend existing open algorithms.

3.2. Localization Algorithm

We decided to only implement open-form solutions because they are more accurate, and it is relatively easy to add additional constraints, which is not the case with closed-form algorithms. However, existing open-form algorithms have a crucial disadvantage. They are designed to operate within Cartesian coordinate space, and the incorporation of nonlinear constraints is a challenge. In this paper, we operate under the assumption of known altitude, which enables the incorporation of an additional constraint to enhance the accuracy of the localization algorithms. However, as previously stated, available algorithms are incapable of incorporating this information. Therefore, we investigate accuracy, and the localization problem is formulated as a standard nonlinear optimization problem. A general-purpose nonlinear solver is used to find a solution. Despite the fact that this paper utilizes only one additional constraint, the incorporation of additional measurements from different sensors is a straightforward process. This makes the method appealing for practical applications.

To localize the aircraft, we formulate nonlinear optimization problems for each case ((4) and (5)), where the goal is to find the lowest possible mean square error (MSE*). In these formulations, $TDOA$ and TOA represent the measurements, \overline{TDOA} and \overline{TOA} represent the most likely measurements given a tuple of positions (with a timestamp while trying to localize directly with TOA measurements), alt is a measurement of altitude, and $a(x, y, z)$ returns an altitude in Geo given its position in ENU or ECEF coordinates. In both optimization formulations, it is possible to eliminate one decision variable by using an $a(x, y, z)$ constraint. This phenomenon can be attributed to the fact that a specific pair of x and y points always permits only one z . In order to further simplify the optimization problem, the other constraint (i.e., the value of \overline{TDOA} or \overline{TOA}) is also eliminated and inserted directly into the cost function.

$$\begin{aligned} \text{MSE}^* &= \min_{x,y,z} \frac{1}{n-1} \sum_{i=2}^n (TDOA_{i,1} - \overline{TDOA}_{i,1}(x,y,z))^2 & (4) \\ &\text{s.t. for } i = 2, \dots, n \\ \overline{TDOA}_{i,1}(x,y,z) &= \frac{1}{c} (||P - \bar{P}_i|| - ||P - \bar{P}_1||) \\ a(x,y,z) &= \text{alt} \end{aligned}$$

$$\begin{aligned} \text{MSE}^* &= \min_{x,y,z,Ts} \frac{1}{n} \sum_{i=1}^n (TOA_{i,1} - \overline{TOA}_{i,1}(x,y,z,Ts))^2 & (5) \\ &\text{s.t. for } i = 1, \dots, n \\ \overline{TOA}_{i,1}(x,y,z,Ts) &= \frac{1}{c} ||P - \bar{P}_i|| + Ts \\ a(x,y,z) &= \text{alt} \end{aligned}$$

It is important to note that knowledge of the altitude does not result in the transformation of a three-dimensional optimization problem into a two-dimensional one. The rationale behind this assertion is that the Earth is not a flat surface; thus, the same values of altitude may possess differing values on the Z-axis within the same Cartesian coordinate system.

As previously mentioned, it is possible to use a general-purpose nonlinear solver (which is convex in the case of three stations and non-convex in the case of more than three stations) to find an optimal tuple. Such solvers can be found in MATLAB's Optimization and Global Optimization Toolboxes and Python's SciPy package (Version: 1.0), among others.

Each of the implemented algorithms is treated as a nonlinear optimization problem, where the position of an aircraft is unknown, and the least-squares solver is used to find the global minimum. In each method, we start by transforming the position of each station in Geo coordinates to ECEF coordinates. A constraint is added to a set of equations to ensure the correct altitude. Once a solution is obtained, we transform it into Geo coordinates.

In the context of optimization problems, the objective is to identify a local minimum of a function. However, when the function is non-convex, it can possess multiple local minima, i.e., there exists an argument for which all values in a nearby region are higher than the found local minimum. Nevertheless, when viewed within the context of the entire environment, a global minimum exists, for which the function value is lower. Local minima may mislead optimization algorithms due to the absence of a mechanism to discern between local and global minima.

In the context of this particular problem, if the optimization problem identifies a global minimum, the location that is returned is the most probable, given the available measurements. In the presentation of the case study (see Section 5 for more details), a comparison of the algorithms is made based on their frequency of reaching the global minimum, among others.

It should be noted that there are methodologies for increasing the probability of finding the global minimum, or at least a local minimum in its neighborhood. The most common methodologies are the multi-start [23] and the initial guess [24]. However, this paper's objective is to evaluate optimization algorithms; therefore, these methodologies are not utilized.

3.3. Influence of the Arrangement of Stations on the Variance of Position Measurement

To compute the measurement error given the aircraft position found by the localization algorithm, we extend the method from [3]. Jacobian (J) matrices are derived based on the chosen method, and (6) is used to compute the GDOP (geometric DOP) value. The original approach from [3] to derive J was designed for three-dimensional problems in which the position is unknown in all three dimensions. However, given that the potential measurement error is typically negligible compared to the size of the environment, it is reasonable to assume that the altitude constraint $a(\cdot)$ is equivalent to a constant value on the z -axis. In such a case, it is possible to employ the same procedure that results in a smaller number of columns, as there is one fewer decision variable.

We use the same equations for the covariance matrix (Q) as those derived in the original source. Note that, although the variance σ^2 appears in (6), it does not affect the result because it is canceled out by the elements of the Q matrix, which consist solely of constant multiples of σ^2 . The covariance matrix is used to show whether the measurements of different ground stations are correlated (TDOA) or not correlated (TOA). To compute the Jacobian given the aircraft position, we transform the position of all stations to ENU coordinates, where the aircraft position is the origin, i.e., $P = [0, 0, 0]$. Also, in this coordinate system, z is parallel to the altitude, so it is possible to treat it as a constant instead of a variable, which means that the Jacobian has one fewer column.

$$GDOP = \sqrt{\text{trace}\left(\frac{1}{\sigma^2}(J^T J)^{-1} J^T Q J (J^T J)^{-1}\right)} \quad (6)$$

The TDOA-based Jacobian is computed by differentiating (2) with the same station as the reference. Different references would give different measurement errors, but for

reasonably placed stations, the change is negligibly small. The Jacobian and covariance matrices can be computed using (7) and (8), respectively.

$$J = \frac{1}{c} \begin{bmatrix} \frac{-\bar{x}_1}{\|\bar{P}_1\|} - \frac{-\bar{x}_2}{\|\bar{P}_2\|} & \frac{-\bar{y}_1}{\|\bar{P}_1\|} - \frac{-\bar{y}_2}{\|\bar{P}_2\|} \\ \vdots & \vdots \\ \frac{-\bar{x}_1}{\|\bar{P}_1\|} - \frac{-\bar{x}_N}{\|\bar{P}_N\|} & \frac{-\bar{y}_1}{\|\bar{P}_1\|} - \frac{-\bar{y}_N}{\|\bar{P}_N\|} \end{bmatrix} \quad (7)$$

$$Q = \begin{bmatrix} 2\sigma^2 & \sigma^2 & \dots & \sigma^2 \\ \sigma^2 & 2\sigma^2 & \dots & \sigma^2 \\ \vdots & \vdots & \ddots & \vdots \\ \sigma^2 & \sigma^2 & \dots & 2\sigma^2 \end{bmatrix} \quad (8)$$

When using range measurements directly (1), the Jacobian and covariance matrices can be computed using (9) and (10), respectively. This simplifies (6) to (11):

$$J = \begin{bmatrix} \frac{-\bar{x}_1}{c\|\bar{P}_1\|} & \frac{-\bar{y}_1}{c\|\bar{P}_1\|} & 1 \\ \vdots & \vdots & \vdots \\ \frac{-\bar{x}_N}{c\|\bar{P}_N\|} & \frac{-\bar{y}_N}{c\|\bar{P}_N\|} & 1 \end{bmatrix} \quad (9)$$

$$Q = \begin{bmatrix} \sigma^2 & 0 & \dots & 0 \\ 0 & \sigma^2 & \dots & 0 \\ \vdots & \vdots & \ddots & \vdots \\ 0 & 0 & \dots & \sigma^2 \end{bmatrix} \quad (10)$$

$$GDOP = \sqrt{\text{trace}((J^T J)^{-1})} \quad (11)$$

The TOAq-based method assumes that the aircraft has responded to our query so that we can estimate the time of sending a message. In this case, the Jacobian can be estimated using (12) and the covariance can be estimated using (10), but it is important to remember that the measurement variance is greater than in other methods due to the additional variance introduced by n_s .

$$J = \frac{1}{c} \begin{bmatrix} \frac{-\bar{x}_1}{\|\bar{P}_1\|} & \frac{-\bar{y}_1}{\|\bar{P}_1\|} \\ \vdots & \vdots \\ \frac{-\bar{x}_N}{\|\bar{P}_N\|} & \frac{-\bar{y}_N}{\|\bar{P}_N\|} \end{bmatrix} \quad (12)$$

Note that the GDOP used to calculate the variance of position measurement represents the minimum attainable measurement variance. Nonetheless, the findings may exhibit reduced precision in practical applications. One potential explanation pertains to physical phenomena, such as the reflection of electromagnetic waves. However, these considerations fall outside the scope of this particular study.

However, it should be noted that any findings related to the DOP are only useful under the assumption that the global minimum has been identified. In the event that the algorithm identifies a local minimum, it is not possible to establish an upper bound between the actual and estimated locations. It must be noted, however, that this phenomenon only occurs in the event that at least four stations are used.

4. Software

We created an application called “MLAT Analyzer” (Version 1.0) [25], designed to help engineers make decisions about where to place ground stations. Existing approaches usually show a perfect arrangement, but in the real world, this may be impossible for

various reasons (e.g., there could be an existing building in the potential location). Instead of calculating a few parameters that try to describe the whole area, the software shows exactly how the GDOP changes over the area (Figure 1). This is especially useful when ground stations monitor locations that are not of equal importance.

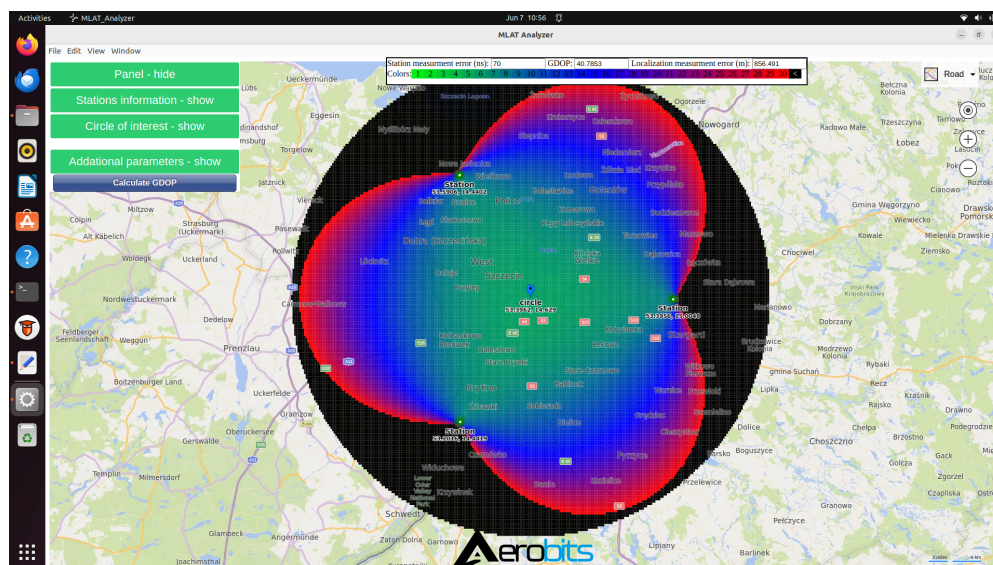


Figure 1. The application demonstrates the variation in the value of the GDOP for the chosen area by selecting the appropriate color: green, blue, red, or black for GDOP values ranging from 1 to 10, from 10 to 20, from 20 to 30, and above 30, respectively. Green dots represent the locations of the ground stations.

The intuitive interface and Bing map-based visualization allow users to quickly test multiple configurations, as shown in Figure 2. By clicking on any of the green buttons, a menu appears, allowing the user to select various parameters. For instance, Figure 3 displays the menu that appears after clicking “Station information-show”. The application enables a variety of functions, including the ability to retrieve information regarding existing stations, modify their positions, deactivate stations (i.e., stations that will not be utilized in computations), or introduce new stations by either clicking on the map or entering text.

Users can access additional parameters, such as selecting a base station and creating an irregular shape for the region of interest. The latter is useful in reducing computation time when a high resolution is selected. These additional parameters can be found in two other menus. By moving the cursor over the region of interest, as shown in Figure 4, the application displays the exact GDOP value. If the user enters the accuracy of the time measurement (in ns), the application displays the accuracy of the position measurement in meters. The application possesses all standard functionalities, including the capacity to save and load the positions of stations to and from files.

We used the Python package (Version: 1.0) [26], in which multiple MLAT solvers can be compared based on accuracy and computation time in a simulation with a moving plane. From the existing literature, we implemented Schau’s algorithm [14], Chan’s algorithm [12], and Foy’s algorithm [7], including the extended Foy algorithm. Foy’s algorithm was extended to work with altitude measurements, and the heaviest computation was compiled as C code.

We also used a general-purpose default nonlinear least-squares solver with SciPy [27], which utilizes the Trust Region Reflective approach to ascertain the optimal solution. It also allows us to easily add bounds and other constraints to the possible locations of the aircraft, which is very useful in the tracking problem when the aircraft has already been localized in the previous iteration.

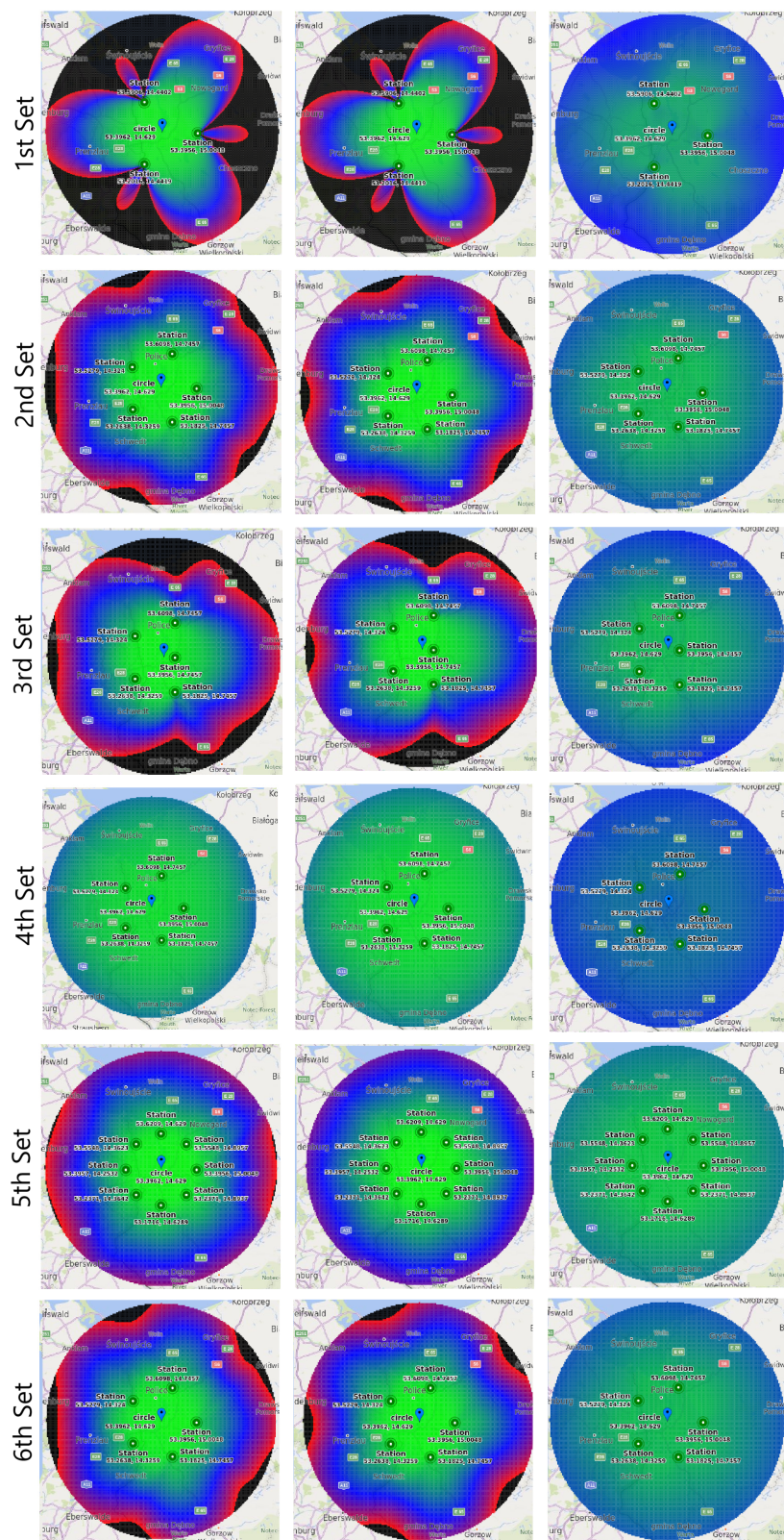


Figure 2. GDOP values of the selected area, given the method and arrangement of stations. Each *i*-th row corresponds to the *i*-th arrangement and shows the results obtained with the TDOA, TOA, and TOAq measurements, in that order. The colors have the same meaning as in Figure 1 for the TDOA and TOA measurements, but the TOAq was rescaled such that the original scale of 1–30 was transformed into 1–6. In the absence of this rescaling, the results obtained through the implementation of TOAq measurements would be challenging to differentiate.

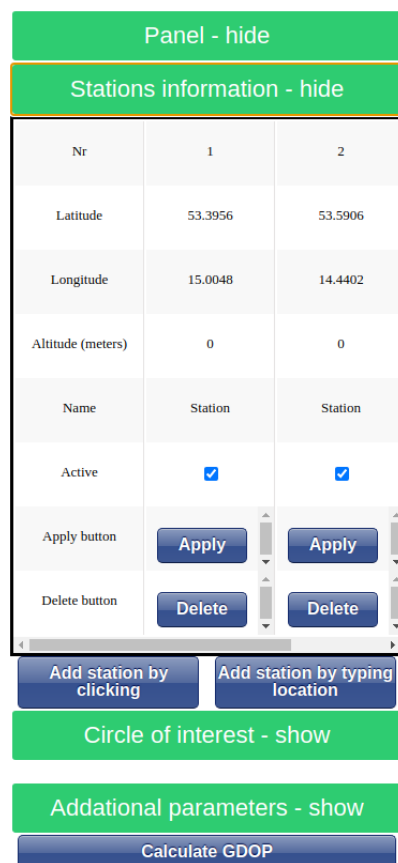


Figure 3. Station placement menu.

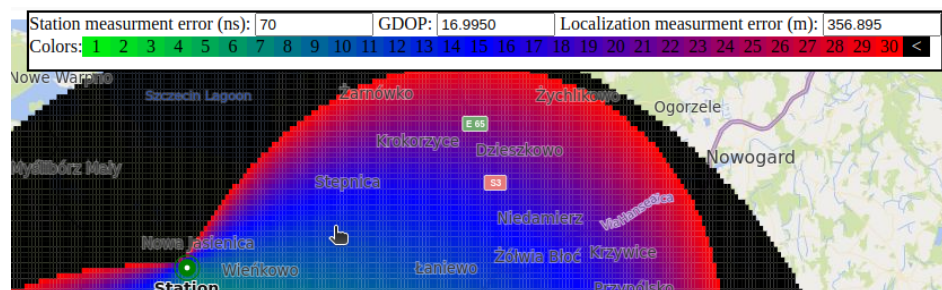


Figure 4. Description of the colors and additional information related to the accuracy of a selected pixel.

5. Experimental Results and Discussion

This section shows the results of the simulation with all assumptions met. We used six different station arrangements. The comparisons between sets of stations placed at the vertices of regular polygons (Tables 2–4) show how the number of stations affects measurement accuracy. The comparisons between sets of five stations arranged differently (Tables 3 and 5) show how irregular placement and station altitude affect the system. A comparison was also made between the effects of altitude on the results, given that the fourth and sixth arrangements are identical to the first, but the altitude of the aircraft and the ground stations differs in the fourth and sixth arrangements, respectively. Also, each time a station receives a signal, it adds normally distributed noise with a variance of 70 ns to the TOA measurement. Note that when ground stations receive a measurement, they are affected by both random noise and constant bias. However, if a designer has access to the stations, it is possible to estimate the bias between stations and take it into account before using the localization algorithm, which allows the constant bias to be ignored.

Table 2. First arrangement: stations are placed in a regular triangle formation.

Lat. [°]	Lon. [°]
53.3956	15.0048
53.5906	14.4402
53.2016	14.4419

Table 3. Second arrangement: stations are placed in a regular pentagon formation.

Lat. [°]	Lon. [°]
53.3956	15.0048
53.6098	14.7457
53.5279	14.3240
53.2638	14.3259
53.1825	14.7445

Table 4. Fifth arrangement: stations are placed in a regular octagon formation.

Lat. [°]	Lon. [°]
53.3956	15.0048
53.5548	14.8957
53.6209	14.6290
53.5548	14.3623
53.3957	14.2532
53.2371	14.3642
53.1716	14.6289
53.2371	14.8937

Table 5. Third arrangement: stations are placed in a trapezoid formation.

Lat. [°]	Lon. [°]
53.3956	14.7457
53.6098	14.7457
53.5279	14.3240
53.2638	14.3259
53.1825	14.7457

To provide a fair evaluation of the performance of the proposed algorithm, a comparison is necessary. However, the open algorithms referenced in Section 2 do not utilize altitude to determine the solution. As the rationale indicates, in instances where a comparison between a proposed algorithm and state-of-the-art methods is implemented without the necessary adjustments, the former will demonstrate a clear advantage. In order to guarantee a fair comparison, it was necessary to extend Foy's algorithm.

Foy's algorithm is a method for finding solutions iteratively (starting from an initial guess) in ENU coordinates (or another Cartesian coordinate system) by updating the position values in three coordinates. In the extended Foy algorithm, the value on the up-axis is constrained, meaning it is treated as constant. Subsequently, the conventional one-step update is employed; however, the Jacobian matrix has one fewer column, resulting

in a reduction of the update to the position on the east and north coordinates. Nevertheless, the implemented constraint is a plane, which is not precisely equivalent to the original constraint of altitude due to the curvature of the Earth. However, it constitutes a rather satisfactory approximation for a minor update.

To rectify the issue, the algorithm transitions from the ENU coordinate system to the geodetic coordinate system. Within the confines of this system, the rectification of altitude is a relatively uncomplicated process. Subsequent to the correction of altitude, the coordinate system undergoes a transformation into the ENU coordinate system once more, this time with the corrected position. As is the case with the original Foy algorithm, the steps are reiterated until convergence is achieved. The idea of this extension was based on Sequential Quadratic Programming [28].

5.1. Measurement Error

We started by calculating a set of GDOP values in the circle with a radius of 80 km. The center of the circle had a latitude of 53.3962 and a longitude of 14.6290. All values were computed using an aircraft moving at an altitude of 1 km and stations placed at an altitude of 0 km. The positions of the stations are specified in Tables 2–5. Two additional station sets are not listed in the tables but have the same arrangement as the second set. The fourth set monitors aircraft moving at an altitude of 50 km. The sixth set includes stations at varying elevations: 0, 200, 500, 200, and 500 m. The results were computed for each pair of methods and arrangements and are shown in Figure 2.

Based on the results, it can be concluded that the TOA from the query always yielded the best GDOP value over the whole area. However, the variance of the measurement was higher, so if the GDOP values are similar to those of other methods, it may be better to use those instead. This may be the case if the user is mainly interested in the middle area between stations.

It is interesting to note that the GDOP values for the TDOA and TOA are always the same when exactly three ground stations are used, which is intuitive since the system is not overdetermined. With more stations, the TOA has the potential to provide better results. Moreover, in the case of three stations, it does not matter which reference station is used to compute the TDOA. However, in the other cases, it does matter. As can be seen, even for stations placed at the vertices of a regular polygon, the GDOP values are not symmetrical because the reference station becomes more important.

For each method, the more stations there are, the more accurate the system becomes. However, the GDOP is strongly influenced by the arrangement of the stations. However, the altitude of the stations is not so important.

As illustrated in Figure 2, the discrepancy is evident in both the TDOA and TOA scenarios, with the GDOP exhibiting significant variations, exceeding 30 in some instances. The TOAq demonstrates nearly indistinguishable behavior, with GDOP values fluctuating from 1 at the center to 3 along the boundaries. This observation highlights the extent to which the accuracy of estimating the information arrival time can be improved before solving the optimization problem.

As demonstrated in the fourth segment, the altitude of the aircraft exerts a substantial influence on the GDOP. The evidence shows that a greater degree of focus should be placed on the arrangement in cases where aircraft are expected to move at relatively low speeds.

5.2. Testing Algorithms

In this section, we compare the raw results obtained by our implementation of the three listed optimization problems (TDOA, TOA, and TOAq) solved using the extended Foy algorithm and the least-squares solver. The results for the TOAq were obtained

twice, with and without additional noise, with a variance of 70 ns. The reason for this is that a clearer comparison between the TOA and TOAq can be made if the measurement noise is the same in both cases. Nonetheless, in actual applications, the requirement of the second message results in a duplication of noise. For this reason, we examined two cases: with and without doubled noise. Although we know the GDOP, it only reflects the correct measurement variance if the algorithm is always able to find the global minimum. Therefore, if open methods are used without an initial guess, it is possible to encounter a much higher error.

In the experiment, we simulated a plane moving at constant speed and altitude. The first measurement was taken at $P = [53.39, 14.68, 5000]$, and the last measurement was taken at $P = [53.71, 15.16, 5000]$ (with the exception of the fourth arrangement, in which the altitude was 10 km). The entire path was divided into four equal parts. The first two parts were within the area enclosed by the stations. For each part, we generated 500 sets of noisy TOA measurements, where the noise was sampled from a normal distribution. We used the same initial estimate, namely the center of the circle of interest from the previous section, i.e., at latitude 53.39624 and longitude 14.62899, for each method and each set of measurements. The results are presented in Table 6.

In the case of three stations, the passive algorithms returned exactly the same solution because there was only one local minimum, i.e., the global minimum. With more stations, the Foy algorithm showed slightly worse results when all algorithms converged to the global minimum, but it almost always converged close to the region around the global minimum. Both passive approaches solved with least squares showed similar performance, but the results obtained by solving the optimization problem directly with the TOAs usually yielded lower error, which is consistent with the results shown in the previous section. The asymmetric placement of the stations not only increased the GDOP but also made it more difficult to find the global minimum. The active algorithms achieved better results when the aircraft was outside the region formed by the ground stations, but even within the region, the results were similar, and it was easy to find the neighborhood of the global minimum. Finally, an enhancement in the aircraft's localization was evident when it was situated at higher altitudes. Although this enhancement was slight in magnitude, its consistency is notable.

Table 6. Errors [m] as a function of the station arrangement, path segment, and algorithm used.

		Foy	TDOA	TOA	TOAq	TOAq with Doubled Noise	
1st Set	1st p.	mean error	23.42	23.42	23.42	22.60	24.03
		median error	21.92	21.92	21.92	21.31	22.30
		std	12.75	12.75	12.75	12.14	13.17
	2nd p.	mean error	35.21	35.21	35.21	21.78	30.35
		median error	30.64	30.64	30.64	19.62	28.23
		std	22.11	22.11	22.11	11.74	15.54
	3rd p.	mean error	71.08	71.08	71.08	22.11	29.34
		median error	60.03	60.03	60.03	20.92	28.51
		std	49.78	49.78	49.78	12.09	14.51
	4th p.	mean error	137.69	137.69	137.69	170.16	162.78
		median error	116.59	116.59	116.59	28.87	36.350
		std	101.28	101.28	101.28	311.92	287.57

Table 6. Cont.

		Foy	TDOA	TOA	TOAq	TOAq with Doubled Noise	
2nd Set	1st p.	mean error	19.46	18.23	17.18	16.70	17.69
		median error	18.36	17.15	16.32	15.75	16.26
		std	9.95	9.37	8.63	8.66	9.30
	2nd p.	mean error	25.31	22.70	22.18	16.82	24.24
		median error	22.22	20.79	20.51	15.43	22.86
		std	14.63	13.00	12.40	8.59	12.83
	3rd p.	mean error	66.52	61.81	60.10	17.55	26.44
		median error	52.99	48.10	48.40	15.97	25.19
		std	49.46	46.62	44.97	9.81	12.97
	4th p.	mean error	152.88	146.88	140.84	22.46	28.79
		median error	127.19	124.32	122.44	20.46	27.45
		std	106.70	102.69	99.64	13.15	14.21
3rd Set	1st p.	mean error	23.04	25.17	21.39	18.84	23.12
		median error	21.75	23.36	20.20	17.33	20.68
		std	11.88	13.29	11.27	9.63	12.67
	2nd p.	mean error	39.05	39.11	36.73	17.97	26.91
		median error	32.88	35.02	32.57	16.44	24.74
		std	25.50	22.55	22.74	9.72	14.58
	3rd p.	mean error	93.77	107.58	92.90	20.29	27.16
		median error	74.07	77.08	74.51	17.67	25.59
		std	71.87	122.25	70.41	12.42	14.19
	4th p.	mean error	188.95	12,780.94	5604.97	530.05	546.09
		median error	145.64	12,712.58	7999.31	634.41	642.35
		std	148.71	2544.31	5342.22	395.89	399.87
4th Set	1st p.	mean error	20.70	20.89	19.28	18.76	19.57
		median error	19.96	19.44	18.15	17.95	18.42
		std	10.41	10.34	9.48	9.28	9.90
	2nd p.	mean error	27.13	24.62	23.85	18.08	25.05
		median error	25.60	22.31	22.17	17.19	23.91
		std	14.73	13.73	13.07	9.37	13.01
	3rd p.	mean error	56.01	51.92	51.02	18.76	26.97
		median error	46.98	44.56	43.01	17.22	26.10
		std	37.36	35.71	36.07	11.07	14.15
	4th p.	mean error	126.58	121.20	116.62	22.62	28.98
		median error	106.19	101.67	98.03	20.10	28.09
		std	88.69	84.69	83.48	13.71	14.47

Table 6. *Cont.*

		Foy	TDOA	TOA	TOAq	TOAq with Doubled Noise	
5th Set	1st p.	mean error	17.49	16.59	13.83	13.53	14.45
		median error	16.53	15.55	13.14	12.65	13.35
		std	9.49	8.85	7.22	7.03	7.62
	2nd p.	mean error	20.30	19.53	16.51	13.77	20.67
		median error	19.16	17.32	14.89	13.12	19.02
		std	11.26	11.53	9.67	7.69	11.24
	3rd p.	mean error	51.13	54.30	1028.13	14.76	24.17
		median error	42.78	43.53	47.65	13.68	23.73
		std	36.91	40.31	2087.79	8.36	11.33
	4th p.	mean error	109.72	10,506.15	11,377.65	18.59	25.95
		median error	94.46	10,468.56	11,352.51	16.10	25.76
		std	75.97	2065.76	2204.58	11.32	12.20
6th Set	1st p.	mean error	19.33	19.08	17.84	17.39	18.43
		median error	17.76	17.99	16.72	16.08	17.84
		std	10.25	9.75	9.04	8.92	9.35
	2nd p.	mean error	25.84	23.61	22.78	17.03	25.44
		median error	13.08	21.02	21.00	15.99	24.37
		std	14.66	13.61	12.93	9.30	12.61
	3rd p.	mean error	61.67	56.30	55.29	17.97	26.61
		median error	51.56	47.37	45.00	16.46	25.47
		std	43.22	39.61	38.70	9.56	13.15
	4th p.	mean error	146.94	140.22	135.59	21.67	28.45
		median error	122.17	112.01	117.12	19.68	27.81
		std	110.30	106.50	101.91	12.80	13.27

6. Conclusions

Solving the MLAT problem is a critical task in various fields such as navigation, telecommunications, and geolocation. This paper has explored various algorithms and their effectiveness in solving the multilateration problem, aiming to design dedicated software that helps users compare these algorithms and determine the best achievable measurement accuracy.

We implemented a series of algorithms that utilize time-difference-of-arrival (TDOA) measurements to determine the position of an aircraft, under the assumption that the aircraft’s altitude is known. We compared the algorithms based on the GDOP, which estimates measurement error in the event that the most optimal algorithm is utilized. Moreover, we tested the results in a simulated environment with a moving aircraft whose real position was known.

The results indicate that the GDOP is influenced by the station arrangement, the number of stations, the algorithm used (when the number of stations exceeds three, i.e., when the system is overdetermined), and primarily by the altitude of the aircraft or knowledge/estimation of the time the information was transmitted.

The results of the simulation indicate that the probability of all algorithms identifying a local minimum rather than a global minimum increases with the number of stations, with this occurrence becoming possible when the number exceeds three. The probability of occurrence of this risk is elevated in the absence of a reliable method for determining the time of transmission of the message, and in the case of a greater distance of the aircraft from the center of the regions under observation. The potential for risk is amplified in scenarios where the aircraft operates in areas outside the designated perimeter surrounding the ground stations.

Nonlinear solvers have been shown to produce more accurate results than Foy's algorithm in most cases. Nevertheless, the extended Foy algorithm demonstrated a notable degree of resilience to errors, particularly in regions beyond the conventional operational scope. This attribute led to its notable superiority in terms of performance compared to the proposed alternative solutions.

It has been demonstrated that, in applications employing a general-purpose nonlinear solver, the utilization of time-of-arrival (TOA) measurements typically yields superior outcomes in comparison to those obtained through time-difference-of-arrival (TDOA) measurements. Active algorithms demonstrate superior performance, even in the presence of additional noise. In such circumstances, the performance of the system is significantly enhanced in areas that are distant from the stations. However, there is a tendency for performance to be marginally compromised in close proximity to the central region of the area under consideration.

Finally, the desktop application allows users to compare different station arrays, which is very important when the possible station locations are limited or the locations in the area of interest are not equally important.

Author Contributions: Conceptualization, R.O.; methodology, R.O. and F.S.; software, F.S.; validation, R.O. and F.S.; formal analysis, F.S.; investigation, R.O. and F.S.; resources, R.O.; data curation, F.S.; writing—original draft preparation, F.S.; writing—review and editing, R.O.; visualization, F.S.; supervision, R.O.; project administration, R.O.; funding acquisition, R.O. All authors have read and agreed to the published version of the manuscript.

Funding: This research received no external funding.

Data Availability Statement: The original contributions presented in this study are included in the article. Further inquiries can be directed to the corresponding author.

Conflicts of Interest: The authors declare no conflicts of interest.

Abbreviations

The following abbreviations are used in this manuscript:

ADS-B	Automatic Dependent Surveillance–Broadcast
alt	Altitude
c	Speed of light
DOAJ	Directory of Open Access Journals
DOP	Dilution of Precision
ECEF	Earth-Centered, Earth-Fixed
ENU	East–North–Up
GDOP	Geometric Dilution of Precision
Geo	Geographic
GPS	Global Positioning System
J	Jacobian matrix
lan	Latitude
lon	Longitude

MLAT	Multilateration
MSE	Mean square error
P	Position vector
Q	Covariance matrix
RMS	Root mean square
Ta	Time needed to answer a query
TDOA	Time difference of arrival
TOA	Time of arrival
TOAq	Time of arrival from query
Tq	Timestamp of sending a query
Ts	Timestamp of sending a message
UAV	Unmanned aerial vehicle

References

1. Figuet, B.; Monstein, R.; Felux, M.T. Combined Multilateration with Machine Learning for Enhanced Aircraft Localization. *Proceedings* **2020**, *10*, 142–149. [[CrossRef](#)]
2. Zhang, F.; Li, H.; Ding, Y.; Yang, S.H.; Yang, L. Dilution of precision for time difference of arrival with station deployment. *IET Signal Process.* **2021**, *105*, 353–364. [[CrossRef](#)]
3. Li, B.; Dempster, A.; Wang, J. 3D DOPs for Positioning Applications Using Range Measurements. *Wirel. Sens. Netw.* **2011**, *3*, 343–349. [[CrossRef](#)]
4. Pei, X.; Huang, Z.; Zhu, Y.; Liu, W. Research on the relationship between DOP and the number of stations for multilateration system. In Proceedings of the 2010 IEEE International Conference on Information Theory and Information Security, Beijing, China, 17–19 December 2010; pp. 786–789.
5. Marzioli, P.; Santoni, F.; Piergentili, F. Evaluation of Time Difference of Arrival (TDOA) Networks Performance for Launcher Vehicles and Spacecraft Tracking. *Aerospace* **2020**, *7*, 151. [[CrossRef](#)]
6. El-Ghoboushi, M.; Ghuniem, A.; Gaafar, A.; Abou-Bakr, H.E. A 2D multilateration algorithm used for air traffic localization and tracking. In Proceedings of the 2018 35th National Radio Science Conference (NRSC), Cairo, Egypt, 20–22 March 2018; pp. 197–204.
7. Foy, W.H. Position-Location Solutions by Taylor-Series Estimation. *IEEE Trans. Aerosp. Electron. Syst.* **1976**, *AES-12*, 187–194. [[CrossRef](#)]
8. Mantilla-Gaviria, I.; Leonardi, M.; Galati, G.; Balbastre, J. Localization algorithms for multilateration (MLAT) systems in airport surface surveillance. *Signal Image Video Process.* **2014**, *9*, 1549–1558. [[CrossRef](#)]
9. Pei, X.; Huang, Z.; Zhang, J.; Zhu, Y.; Liu, W. An approach for close-form solution of multilateration equations. In Proceedings of the 2010 8th World Congress on Intelligent Control and Automation, Jinan, China, 7–9 July 2010; pp. 5464–5478.
10. Schmidt, R.O. A New Approach to Geometry of Range Difference Location. *IEEE Trans. Aerosp. Electron. Syst.* **1972**, *AES-8*, 821–835.
11. Chan, Y.T.; Ho, K.C. A simple and efficient estimator for hyperbolic location. *IEEE Trans. Signal Process.* **1994**, *42*, 1905–1915. [[CrossRef](#)]
12. Ho, K.C.; Kovavisaruch, L.; Parikh, H. Source localization using TDOA with erroneous receiver positions. In Proceedings of the 2004 IEEE International Symposium on Circuits and Systems, Vancouver, BC, Canada, 23–26 May 2004; Volume 3, pp. III–453.
13. bel, J.; Smith, J. The spherical interpolation method for closed-form passive source localization using range difference measurements. In Proceedings of the ICASSP '87. IEEE International Conference on Acoustics, Speech, and Signal Processing, Dallas, TX, USA, 6–9 April 1987; Volume 12, pp. 471–474.
14. Schau, H.; Robinson, A. Passive source localization employing intersecting spherical surfaces from time-of-arrival differences. *IEEE Trans. Acoust. Speech Signal Process.* **1987**, *35*, 1223–1225. [[CrossRef](#)]
15. Mantilla-Gaviria, I.; Leonardi, M.; Galati, G.; Balbastre, J. Time-difference-of-arrival regularised location estimator for multilateration systems. *Radar Sonar Navig. IET* **2014**, *8*, 479–489. [[CrossRef](#)]
16. Galati, G.; Leonardi, M.; De Marco, P.; Menè, L.; Magarò, P.; Gasbarra, M. New Time of Arrival Estimation Method for Multilateration Target Location. In Proceedings of the JISSA'05, Paris, France, 20–21 June 2005.
17. Mantilla-Gaviria, I.; Leonardi, M.; Balbastre, J.; Reyes, E. On the application of singular value decomposition and Tikhonov regularization to ill-posed problems in hyperbolic passive location. *Math. Comput. Model.* **2013**, *57*, 1999–2009. [[CrossRef](#)]
18. Shehu, Y. Aircraft Position Estimation Comparison of Multilateration System Lateration Algorithms with Different Reference Selection Techniques. *ELEKTRIKA-J. Electr. Eng.* **2019**, *18*, 16–21. [[CrossRef](#)]
19. Lee, H.B. A Novel Procedure for Assessing the Accuracy of Hyperbolic Multilateration Systems. *IEEE Trans. Aerosp. Electron. Syst.* **1975**, *AES-11*, 2–15. [[CrossRef](#)]

20. Kaya, F.; Saritas, M. A Computer Simulation of Dilution of Precision in the Global Positioning System Using Matlab. In Proceedings of the 4th International Conference on Electrical and Electronic Engineering, Bursa, Turkey, 7–11 December 2005.
21. Frisch, D.; Li, K.; Hanebeck, U.D. Optimal Sensor Placement for Multilateration Using Alternating Greedy Removal and Placement. In Proceedings of the 2022 IEEE International Conference on Multisensor Fusion and Integration for Intelligent Systems (MFI), Bedford, UK, 20–22 September 2022; pp. 1–6.
22. Hirsch, M. PyMap3D: 3-D coordinate conversions for terrestrial and geospace environments. *J. Open Source Softw.* **2018**, *3*, 580. [[CrossRef](#)]
23. György, A.; Kocsis, L. Efficient Multi-Start Strategies for Local Search Algorithms. *J. Artif. Intell. Res.* **2014**, *41*, 407–444. [[CrossRef](#)]
24. Casella, F.; Bachmann, B. On the choice of initial guesses for the Newton-Raphson algorithm. *Appl. Math. Comput.* **2021**, *398*, 125991. [[CrossRef](#)]
25. Surma, F.; Osypiuk R. *MLAT Application—An Application Designed to Visualize Accuracy of MLAT Measurements over Large Areas, Version 1.0*; Aerobits: Szczecin, Poland, 2024. Available online: <https://data.4tu.nl/datasets/955dfd5a-1270-46e7-8c9c-398469cd56ad/1> (accessed on 19 November 2024).
26. Surma, F.; Osypiuk R. *Solver for MLAT Localization Problem + Tracking Software, Version 1.0*; Aerobits: Szczecin, Poland, 2024. Available online: <https://data.4tu.nl/datasets/996cb843-1d08-4740-8ac0-f59146c47ce8> (accessed on 19 November 2024).
27. Virtanen, P.; Gommers, R.; Oliphant, T.E.; Haberland, M.; Reddy, T.; Cournapeau, D.; Burovski, E.; Peterson, P.; Weckesser, W.; Bright, J.; et al. SciPy 1.0: Fundamental Algorithms for Scientific Computing in Python. *Nat. Methods* **2020**, *17*, 261–272. [[CrossRef](#)] [[PubMed](#)]
28. Boggs, P.; Tolle, J. Sequential Quadratic Programming. *Acta Numer.* **1995**, *4*, 1–51. [[CrossRef](#)]

Disclaimer/Publisher’s Note: The statements, opinions and data contained in all publications are solely those of the individual author(s) and contributor(s) and not of MDPI and/or the editor(s). MDPI and/or the editor(s) disclaim responsibility for any injury to people or property resulting from any ideas, methods, instructions or products referred to in the content.